

# The heterogeneous multiscale method based on the discontinuous Galerkin and the finite volume methods for hyperbolic problems

Shanqin Chen<sup>a</sup>, Weinan E<sup>b</sup>, Chi-Wang Shu<sup>a,\*</sup>

<sup>a</sup> *Division of Applied Mathematics, Brown University, Providence, RI 02912, USA*

<sup>b</sup> *Department of Mathematics, Princeton University, Princeton, NJ 08544, USA*

---

## Abstract

In this paper, we review a discontinuous Galerkin (DG) method and develop a finite volume (FV) method, within the framework of the heterogeneous multiscale method (HMM), for solving hyperbolic problems. Although the methods can be applied to general cases, we consider in this paper only hyperbolic scalar advection equations and Euler systems. Error estimates are given for the linear equations and numerical results are provided for the linear and nonlinear problems to demonstrate the capability of the methods.

*Keywords:* Heterogeneous multiscale method; Homogenization; Discontinuous Galerkin method; Finite volume method; Advection equation; Euler equations

---

## 1. Introduction

In this paper, we review a discontinuous Galerkin (DG) method [1] and develop a finite volume (FV) method, within the framework of the heterogeneous multiscale method (HMM), for solving multiscale hyperbolic problems. The methodology can be applied to general cases (multidimensions, other types of equations, etc.), but we consider in this paper only one-dimensional hyperbolic linear scalar advection equations and nonlinear Euler equations, all with coefficients involving different scales. Direct numerical treatments of these problems are difficult due to the cost required for resolving the smallest scale.

The main motivation behind the HMM is to make efficient usage of both the macroscopic and the microscopic formulations, even in cases when the macroscopic equations or models are not known explicitly. The basic set-up is as follows [2]: We have a microscopic process that describes the microscopic state variable  $u$ , which is defined on a microscopic domain  $\mathcal{D}$ . We also have a macroscopic process that describes the macroscopic state variable  $U$ , which is defined on a macroscopic domain  $D$ . The two processes and state variables are related to each other by the compression and

reconstruction operators, denoted by  $Q$  and  $R$ , respectively:  $Qu = U$ ,  $RU = u$ , with the property  $QR = I$ , where  $I$  is the identity operator. For example, if the microscopic process is described by kinetic theory and the macroscopic process is described by hydrodynamics, then the compression operator maps the one-particle phase-space distribution function to the conserved mass, momentum, and energy densities. The reconstruction operator does the opposite and is, in general, not unique. Our aim is to approximate accurately the macroscopic state of the system. We do so by working with a macroscopic grid that resolves the large scale of the problem. There are two main components in HMM: an overall macroscopic scheme for  $U$  and estimating the missing macroscopic data from the microscopic model.

The main numerical work will consist in solving the microscopic model, but this is only done on small subdomains of the original domain, to a microscopic time that is typically much smaller than the macroscopic time step. Since the microscopic cell problems are independent, they can be solved in parallel, which is another advantage of this method.

In Section 2, we describe the HMM-DG and the HMM-FV methods for the one-dimensional linear hyperbolic scalar advection problem and provide an error estimate and numerical examples. In Section 3, one-dimensional hyperbolic nonlinear Euler systems are considered, where numerical examples are provided.

---

\* Corresponding author. Tel.: +1 401 863 2549; Fax: +1 401 863 1355; E-mail: shu@dam.brown.edu

## 2. Hyperbolic scalar problem

Consider the following model problem in one dimension

$$\begin{aligned} u_t^\varepsilon + (a^\varepsilon(x)(u^\varepsilon)_x) &= 0 \quad \text{in } [0, T] \times [0, 2\pi], \\ u^\varepsilon(x, 0) &= u_0(x) \quad x \in [0, 2\pi], \quad u^\varepsilon(0, t) = u^\varepsilon(2\pi, t) \\ t &\in [0, T] \end{aligned} \quad (1)$$

where  $a^\varepsilon(x)$  is an oscillatory function involving a small scale  $\varepsilon$ . For the analysis, we take the example  $a^\varepsilon(x) = a^\varepsilon(x) = a(x, \frac{x}{\varepsilon}) > 0$ , with  $a(x, y)$  smooth and periodic in  $y$  with a period  $F^\varepsilon = [0, 2\pi]$ , although the methodology can be applied to a general  $a^\varepsilon(x)$ . Classical homogenization theory tells us that  $u^\varepsilon \rightarrow \bar{u}$  weakly in  $L^2((0, T); H_p^1)$ , where  $\bar{u}$  is the solution of the so-called homogenized problem

$$\bar{u}_t + (\bar{a}(x)\bar{u})_x = 0 \quad \text{in } [0, T] \times [0, 2\pi] \quad (2)$$

and  $\bar{a}(x)$  is the harmonic average of  $a^\varepsilon(x) = a(x, \frac{x}{\varepsilon})$  given by

$$\bar{a}(x) = \frac{1}{\frac{1}{2\pi} \int_0^{2\pi} a(x, y)^{-1} dy} \quad (3)$$

The macroscale model for this problem will be

$$U_t + F(U, x)_x = 0 \quad (4)$$

where  $F(U, x) = \bar{a}(x)U$ , but in the HMM-DG and HMM-FV methods we do not assume explicit knowledge of this flux.

### 2.1 Setup of the numerical scheme

We describe only the setup of the HMM-FV method, and refer to Chen, E, and Shu [1] for the setup of the HMM-DG method. The finite volume scheme for Eq. (4) is

$$\frac{dU_j}{dt} = -\frac{F_{j+\frac{1}{2}}^- - F_{j-\frac{1}{2}}^-}{\Delta x_j} \quad (5)$$

for  $j = 1, \dots, N$ , where  $U_j$  approximates the cell averages of the exact solution  $U$  of Eq. (4). Notice that we have chosen the flux  $\hat{F}(U, x)$  to be  $F^- \equiv F(U^-, x)$ , since  $a(x, y) > 0$ , and therefore  $\bar{a} > 0$ . If  $a(x, y)$  is not always positive, then a Lax–Friedrich flux involving both  $U^-$  and  $U^+$  can be used.

The missing data for the finite volume method are  $F_{j\pm\frac{1}{2}}^-$ . We summarize the numerical procedure in the following:

1. Select the microcells: we can pick  $F_{j+\frac{1}{2}}^\varepsilon = [x_{j+\frac{1}{2}} - 2\pi\varepsilon, x_{j+\frac{1}{2}}]$  for the point  $x_{j+\frac{1}{2}}$ .
2. Reconstruct the initial condition for the microscale problem (third-order finite volume reconstruction):  $\hat{u}_0^\varepsilon = U_{j+\frac{1}{2}}^- = -\frac{1}{6}U_{j-1} + \frac{5}{6}U_j + \frac{1}{3}U_{j+1}$ .
3. Solve the microscale problem Eq. (1) on  $F_{j+\frac{1}{2}}^\varepsilon$  with the initial condition  $\hat{u}_0^\varepsilon$  and a periodic boundary condition. We evolve the microstate  $\hat{u}^\varepsilon(t)$  for some suitably chosen time  $T^\varepsilon$ . At each micro-time step, we compute the microscale flux  $\hat{f}^\varepsilon(x, t) = a(x, \frac{x}{\varepsilon})\hat{u}^\varepsilon(x, t)$ , and perform:
4. (a) temporal averaging

$$\hat{f}^\varepsilon(x) = \frac{1}{T^\varepsilon} \int_0^{T^\varepsilon} K(\frac{t}{T^\varepsilon}) \hat{f}^\varepsilon(x, t) dt$$

$$\text{where } K(t) = 1 - \cos(2\pi t).$$

- (b) spatial averaging

$$\hat{F}_{j+\frac{1}{2}}^\varepsilon = F_{j+\frac{1}{2}}^- = \frac{1}{|F_{j+\frac{1}{2}}^\varepsilon|} \int_{F_{j+\frac{1}{2}}^\varepsilon} \hat{f}^\varepsilon(x) dx \quad (7)$$

5. Use Eq. (5) to compute  $U^{m+1}(x)$ .

### 2.2. $L_2$ error estimate

*Proposition 2.1:* Let  $\bar{u}$  be the exact solution of the homogenized problem Eq. (2) and  $U$  be the numerical HMM-FV solution of Eq. (4) using  $(k + 1)$ th order reconstruction in Step 2; then we have the  $L_2$  error estimate

$$\|U - \bar{u}\| \leq C \left( \frac{\varepsilon}{\Delta x} + \frac{\varepsilon}{T^\varepsilon \Delta x} + \Delta x^{k+1} \right) \quad (8)$$

where  $T^\varepsilon$  is the terminal time on the microscale problem and  $C$  is a constant independent of  $\varepsilon$  and of  $\Delta x$  and dependent on the derivatives of  $\bar{u}$ . A similar error estimate is also valid for the HMM-DG method [1].

### 2.3. Numerical results

In this subsection, we present numerical results of the HMM-FV method for Eq. (1) with the initial condition  $u_0(x) = \sin(x)$ . Table 1 contains the  $L_1$  and  $L_\infty$  errors and orders of accuracy when the third-order HMM-FV method is applied to Eq. (1) with the coefficient  $a^\varepsilon(x) = \frac{1}{3 + \sin(x/\varepsilon) + \sin(x)}$ , using  $N$  uniform cells, at  $T = 6.28$ . The microscale problem is solved by the first-order finite volume method using 20 uniform cells and with  $T^\varepsilon = 1000\Delta t^\varepsilon$ , where  $\Delta t^\varepsilon$  is the time step on the microscale problem. We can clearly see third-order accuracy and the dependency between the smallest  $\Delta x$  to observe the correct order and  $\varepsilon$ , agreeing with the

Table 1  
Third-order HMM-FV scheme, first-order FV on microscale,  
 $T = 6.28, a^\varepsilon = \frac{1}{3+\sin(x)+\sin(x/\varepsilon)}$

$\varepsilon$	$N$	$L_1$ error	$L_1$ order	$L_\infty$ error	$L_\infty$ order
$10^{-3}$	9	1.10E-01	–	3.82E-01	–
	19	2.72E-02	1.88	1.40E-01	1.34
	29	2.27E-02	0.42	8.30E-02	1.24
$10^{-6}$	19	2.94E-02	–	1.55E-01	–
	38	5.30E-03	2.47	4.11E-02	1.92
	76	7.51E-04	2.82	7.06E-03	2.54
	152	1.01E-04	2.89	8.30E-04	3.09
	304	4.14E-05	1.29	1.97E-04	2.08
$10^{-9}$	19	2.93E-02	–	1.55E-01	–
	38	5.30E-03	2.47	4.10E-02	1.92
	76	7.51E-04	2.82	7.06E-03	2.54
	152	1.01E-04	2.89	8.30E-04	3.09
	304	1.26E-05	3.05	1.27E-04	3.32
	608	1.59E-06	2.98	1.59E-05	3.00
	1216	2.79E-07	2.51	2.02E-06	2.98

error estimate in Eq. (8). Numerical results for the HMM-DG method can be found in Chen, E, and Shu [1].

### 3. Hyperbolic Euler systems

We consider the Euler equation of compressible gas dynamics

$$u_t^\varepsilon + f(u^\varepsilon)_x = 0, \tag{9}$$

where  $u^\varepsilon = [\rho^\varepsilon, \rho^\varepsilon v^\varepsilon, E^\varepsilon]^T, f(u^\varepsilon) = [\rho^\varepsilon v^\varepsilon, \rho^\varepsilon (v^\varepsilon)^2 + p^\varepsilon, v^\varepsilon (E^\varepsilon + p^\varepsilon)]^T$ , and as a prototype problem we consider the equation of state as involving an oscillatory coefficient

$$p^\varepsilon = a^\varepsilon(x) [(E^\varepsilon - \frac{1}{2} \rho^\varepsilon (v^\varepsilon)^2) (\gamma - 1)]. \tag{10}$$

The harmonic average of  $a^\varepsilon(x) = a(x, x/\varepsilon)$  takes the form of Eq. (3). The simple average of  $a^\varepsilon(x)$  is simply  $\tilde{a}(x) = \frac{1}{2\pi} \int_0^{2\pi} a(x, y) dy$ . The HMM-FV method for the hyperbolic system is formulated in exactly the same fashion as that for the scalar problem, repeated three times for each of the three components of  $u^\varepsilon$ , except for Step 2, where we use the fifth-order WENO reconstruction [3], since this nonlinear problem has shocks in its solution.

#### 3.1. Numerical results

The first numerical example is the nonlinear Euler Eqs. (9) and (10), with the oscillatory coefficient  $a^\varepsilon(x) = \frac{1}{1+0.1\sin(x/\varepsilon)+0.1\sin(x)}$ , the initial condition  $\rho = 1 +$

$0.2 \sin(x), v = p = 1$ , and with periodic boundary conditions. We compute the solution to  $T = 1$ .

We use the finite volume method with a fifth-order weighted essentially non-oscillatory (WENO) reconstruction. The microscale problem is solved by a third-order finite volume method using 20 uniform cells and with  $T^\varepsilon = 1000\Delta t^\varepsilon$ . The HMM-FV solutions with  $N = 38$  and  $N = 76$  uniform cells for  $\varepsilon = 10^{-6}$ , as well as the ‘converged’ local average solution  $\bar{u} = \lim_{\varepsilon \rightarrow 0} \bar{u}^\varepsilon$ , where  $\bar{u}^\varepsilon$  is the local average of  $u^\varepsilon$ , the solution of the oscillatory Euler Eqs. (9) and (10) obtained by a direct numerical simulation of the microscale problem in Eqs. (9) and (10) using the fifth-order WENO scheme [3] with an extremely refined mesh containing at least 20 grid points per period of the  $\varepsilon$  scale structure, are plotted in Fig. 1 (top two figures). We also plot the solution  $\bar{u}$ , the solution of the large-scale equation with  $a^\varepsilon(x)$  in Eq. (10) replaced by a simple average  $\tilde{a}(x)$ , on the same figure. It can be seen clearly, especially in the right-hand figure, which is a zoomed version, that the HMM-FV solutions converge to  $\bar{u}$  rather than to  $\tilde{u}$ , indicating that the HMM strategy is working in this nonlinear case.

The second numerical example is the Sod’s shock tube problem for the nonlinear Euler Eqs. (9) and (10), with the oscillatory coefficient  $a^\varepsilon(x) = \frac{1}{1+0.4\sin(2\pi x/\varepsilon)+0.1\sin(x)}$ , and the initial condition  $\rho = 1, v = 0, p = 1$  if  $x \in [-3,0]$ ;  $\rho = 0.9, v = 0, p = 0.9$  if  $x \in [0,3]$ . We compute the solution to  $T = 0.4$ .

The bottom two figures in Fig. 1 are the HMM-FV solutions for  $N = 19, 38$ , and 76 uniformly spaced mesh cells for  $\varepsilon = 10^{-6}$ , as well as the converged local average solution  $\bar{u}$ . We also plot the solution  $\tilde{u}$  on the same figure as a reference. It can be seen again, especially in the right-hand figure, which is a zoomed version, that the HMM-FV solutions converge to  $\bar{u}$  rather than to  $\tilde{u}$ , indicating that the HMM strategy is again working in this nonlinear case.

### 4. Acknowledgments

The research of S. Chen (x) is supported in part by National Science Foundation (NSF) grant DMS-0207451. The research of C.-W. Shu is supported in part by Army Research Office (ARO) grant W911NF-04-1-0291, NSF grant DMS-0207451, and Air Force Office of Scientific Research (AFOSR) grant F49620-02-1-0113.

### References

[1] Chen S, E W, Shu C-W. The heterogeneous multi-scale method based on discontinuous Galerkin method for hyperbolic and parabolic problems. Accepted by

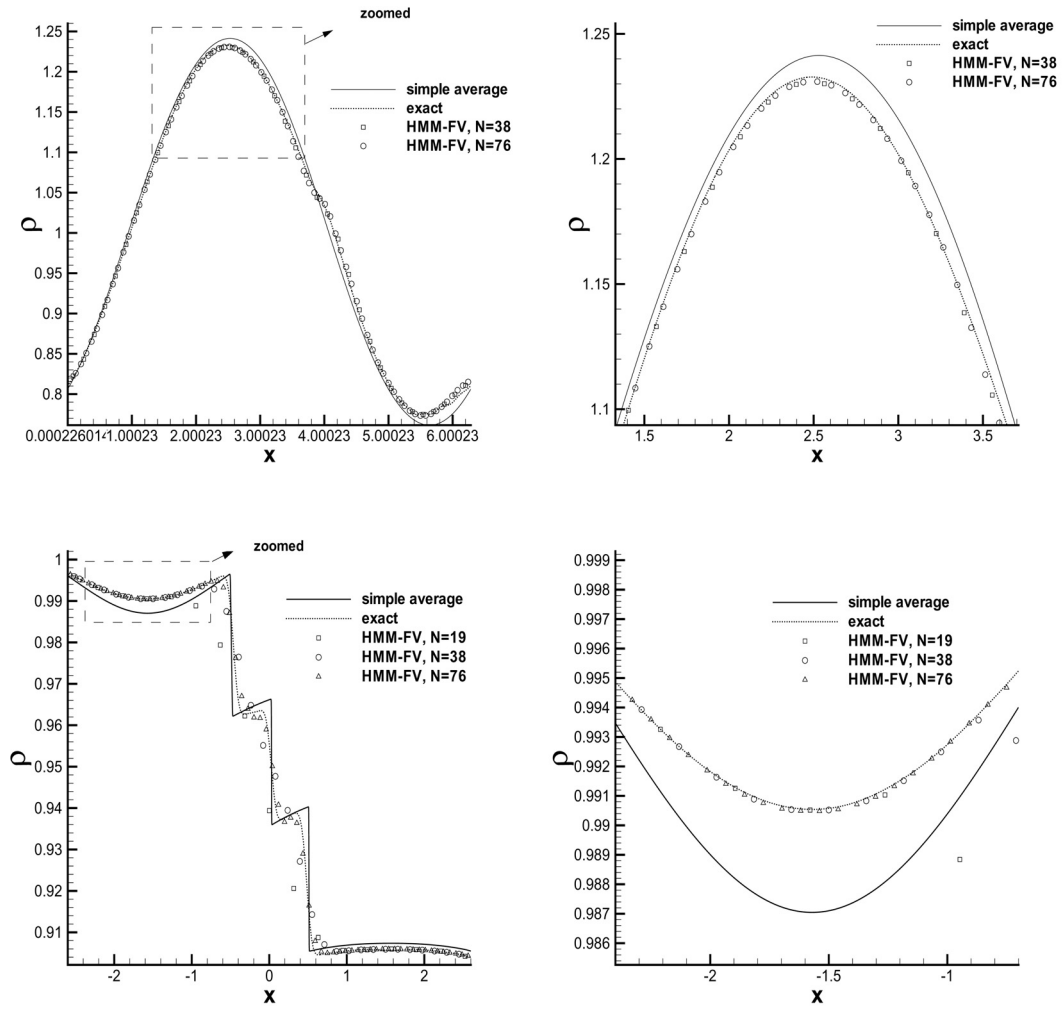


Fig. 1. Density  $\rho$ . Top: the HMM-FV solution with  $N = 38$  and  $76$  uniform cells for  $\varepsilon = 10^{-6}$ , versus the locally averaged solution  $\bar{u}$  to the nonlinear oscillatory Euler equations (denoted by 'exact'). The solution  $\tilde{u}$  of the simply averaged Euler equations (denoted by 'simple average') is also plotted as a reference. Bottom: Sod's Shock tube problem. The HMM-FV solution with  $N = 19, 38,$  and  $76$  uniform cells for  $\varepsilon = 10^{-6}$ , versus the locally averaged solution  $\bar{u}$  to the nonlinear oscillatory Euler equations. The solution  $\tilde{u}$  of the simply averaged Euler equations is also plotted as a reference.

Multiscale Modeling Simulation. A SIAM Interdisciplinary Journal.

[2] E W, Engquist B. The heterogeneous multi-scale methods. Commun Math Sci 2003;1:87–132.

[3] Jiang G, Shu C-W. Efficient implementation of weighted ENO schemes. J Computat Phys 1996;126:202–228.